B-B Coupling

DOI: 10.1002/ange.201304382

Dehydrogenative Boron Homocoupling of an Amine-Borane**

Heather C. Johnson, Claire L. McMullin, Sebastian D. Pike, Stuart A. Macgregor, and Andrew S. Weller**

Dedicated to Professor Larry Sneddon

The dehydrogenative coupling of amine-boranes as catalyzed by transition-metal fragments offers the potential for controlled hydrogen release and the formation of oligomeric and polymeric materials in which head-to-tail coupling yields products with B–N bonds that are isoelectronic with technologically pervasive polyolefins.[1–3] Because of this, the area has received considerable attention recently and there are now a wide range of catalysts available, which operate using inner-sphere- or outer-sphere-type mechanisms,[4] that dehydrogenatively couple amine-boranes of the general formula $H_3B{\cdot}NRR'H$ (R, R′ = H, alkyl) to give monomeric, cyclic, or polymeric amino-borane materials based on $H_2B{=}NRR'$. By contrast, the homocoupling[5] of amine-boranes to form well-defined products with B–B single bonds has not been reported, although dehydrogenation of $H_3B{\cdot}NH_3$ by $[Pd(NCMe)_4][BF_4]$ has been reported to form insoluble polymeric materials with B–B bonds.[6] This preference for heterocoupling likely stems from the fact that B-H/N-H activation of amine-boranes gives amino-boranes that are well set up for further oligomerization through the formation of dative B–N bonds, a process that is also driven thermodynamically by the differences in relative σ-bond strengths between B–B (70 kcal mol^{-1}) and B–N (107 kcal mol^{-1}) single bonds. Well-defined homocoupling of boranes, as mediated by transition metals, is essentially limited to B–B bond formation in polyhedral boranes, for example pentaborane(9) (A),[7,8] guanidine bases (B),[9] and most recently the homocoupling of HBCat and related derivatives to give the corresponding diboranes (C)[10–12] (Scheme 1). By contrast, the homocoupling of phosphines or silanes is well established.[13,14]

The homocoupling of boranes requires the B-H activation of two boranes at a metal center; we, and others, have recently reported on B-H activation at group 9 metal centers in both amine- and amino-boranes.[15,16] In particular, $H_3B{\cdot}NMe_3$ undergoes B-H activation at $\{Rh(PR_3)_n\}^+$ fragments to give bimetallic hydrido-boryl products ($n = 1$, $R_3 = Cy_3$),[17] or in the presence of the alkene *tert*-butylethene (TBE, $n = 2$, $R_3 = i\text{Bu}_2t\text{Bu}$) catalytic hydroboration occurs to afford $Me_3N{\cdot}BH_2CH_2CH_2t\text{Bu}$, **I**.[18] The suggested mechanism for this process involves reversible B-H activation to give a hydrido-boryl complex, alkene insertion, and subsequent reductive elimination of **I**. Homocoupling of $H_3B{\cdot}NMe_3$ was not observed, possibly because the approach of the second equivalent of $H_3B{\cdot}NMe_3$ to the metal is hindered. However, the Ir pincer system $Ir(t\text{BuPOCOP}t\text{Bu})(H)_2$ [tBuPOCOPtBu = $\kappa^3_{P,C,P}$-1,3-$(OPt\text{Bu}_2)_2C_6H_3$] catalyzes the dehydropolymerization of $H_3B{\cdot}NMeH_2$, for which polymer growth kinetics suggest a coordination insertion mechanism consistent with the activation of two amine-boranes at the metal center before B–N bond formation.[3] Taking clues from this and using a related pincer system based on the $\{Rh(Xantphos)\}^+$ fragment,[19] we now report that $H_3B{\cdot}NMe_3$ undergoes stoichiometric homo-dehydrocoupling to form the diborane(4) $H_4B_2{\cdot}2NMe_3$ **II** (Scheme 1D), a compound previously synthesized from the combination of NMe_3 with B_3H_7L (L = THF, SMe_2).[20]

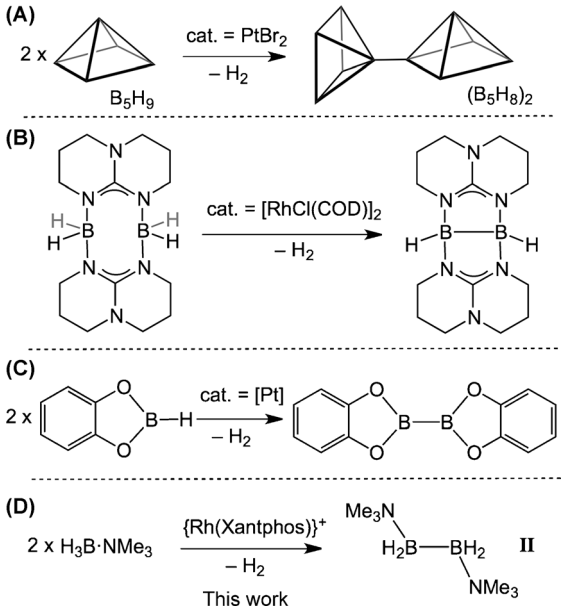

Scheme 1. Homocoupling to form B–B bonds.

Addition of $H_3B{\cdot}NMe_3$ to the precursor $[Rh(\kappa^2_{P,P}\text{-Xantphos})(NBD)][BAr^F_4]$[21] under a H_2 atmosphere resulted in rapid hydrogenation of the diene and coordination of the amine-borane to the resulting Rh^{III} dihydride to give

[*] H. C. Johnson, S. D. Pike, Prof. A. S. Weller
Department of Chemistry, University of Oxford
Mansfield Road, Oxford, OX1 3TA (UK)
E-mail: andrew.weller@chem.ox.ac.uk
Dr. C. L. McMullin, Prof. S. A. Macgregor
School of Engineering & Physical Sciences
Institute of Chemical Sciences, Heriot-Watt University
Edinburgh, EH14 4AS (UK)
E-mail: s.a.macgregor@hw.ac.uk

[**] We thank the EPSRC for funding.
Supporting information for this article is available on the WWW under http://dx.doi.org/10.1002/anie.201304382.

$[Rh(\kappa^3_{P,O,P}\text{-Xantphos})(H)_2(\eta^1\text{-}H_3B{\cdot}NMe_3)][BAr^F_4]$, **2**, in essentially quantitative yield as measured by NMR spectroscopy (Scheme 2). Complex **2** was also characterized by single-crystal X-ray diffraction (Figure 1), which demonstrates a pseudo octahedral Rh^{III} center with an $H_3B{\cdot}NMe_3$ ligand

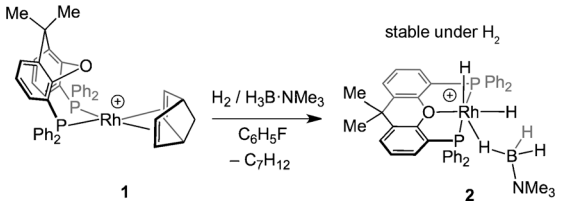

Scheme 2. Synthesis of complex **2**. $[BAr^F_4]^-$ anions not shown.

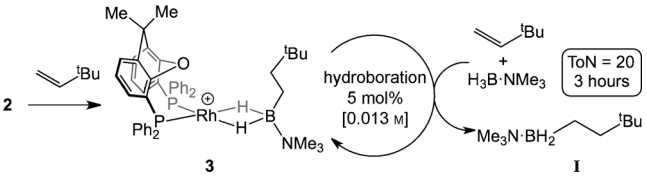

Scheme 3. Complex **3** and the catalytic hydroboration of TBE. $[BAr^F_4]^-$ anions not shown.

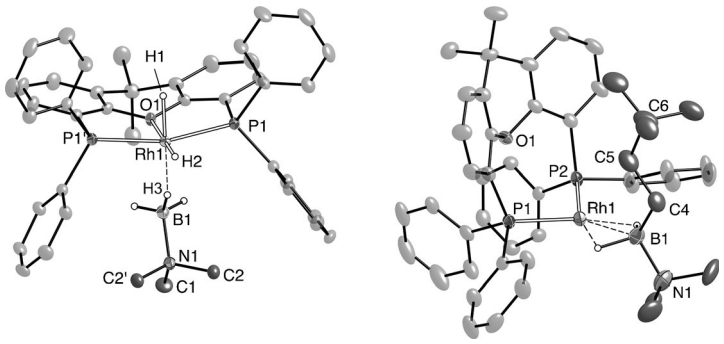

Figure 1. Displacement ellipsoid plots (30%) of the cationic portion of **2** (left) and **3** (right). Only one of the two independent cations in the unit cell is shown for **2** and a crystallographically imposed mirror plane bisects each cation. All carbon-bound hydrogen atoms are omitted for clarity. Selected bond lengths (Å): **2:** Rh1–P1, 2.2683(10); Rh1–O1, 2.199(3); Rh1–B1, 2.759(6); Rh1–H3, 1.759; B1–N1, 1.609(8). **3:** Rh1–P1, 2.2678(12); Rh1–P2, 2.2494(12); Rh1–O1, 3.431(3); Rh1–B1, 2.162(5); B1–N1, 1.604(4).

coordinated through a single Rh-H-B interaction (Rh1–B1, 2.759(10) Å), and a *mer*-κ^3 Xantphos ligand (Rh1–O1, 2.199(3) Å).[22] Complex **2** is closely related to acetone and NCMe adducts such as $[Rh(\kappa^3_{P,O,P}\text{-Xantphos})(H)_2(NCMe)][BAr^F_4]$.[21] The solution NMR data (Supporting Information) are in full accord with the solid-state structure and are consistent with the η^1-coordination mode of the borane.[23] The combined NMR and structural data also suggest that the borane is only weakly bound, and consistent with this it can be liberated by addition of NCMe to **2** to form the corresponding adduct (see above).[21] Complex **2** is a rare example of an amine-borane complex with a pincer-type ligand,[24] although a simple borane adduct $Ir(H)_2(t\text{BuPOCOP}t\text{Bu})(BH_3)$ has been described,[25] and a related silane complex is also known.[26] Complex **2** does not react with additional $H_3B{\cdot}NMe_3$, remaining unchanged upon addition of 20 equivalents under a H_2 atmosphere.

Complex **2** is unstable when not under an atmosphere of H_2, slowly decomposing to give unidentified materials, presumably through the loss of H_2 to give a Rh^I amine-borane species that undergoes B-H activation to a Rh^{III} hydrido-boryl, which is unstable in the absence of excess $H_3B{\cdot}NMe_3$. To probe this, addition of two equivalents of alkene TBE to **2** results in rapid (less than 15 minutes) anti-Markovnikov hydroboration of the alkene to form $[Rh(\kappa^2_{P,P}\text{-Xantphos})(\eta^2\text{-}Me_3N{\cdot}H_2BCH_2CH_2t\text{Bu})][BAr^F_4]$ **3**, in which the resulting alkyl borane **I** interacts with a Rh^I center through two Rh-H-B interactions (Scheme 3). Figure 1 shows the solid-state structure of **3**, and solution spectroscopic data are in full accord with this and are very similar to those reported previously for coordination of this borane with the $\{Rh(Pi\text{Bu}_2t\text{Bu})_2\}^+$ fragment, a complex that is also formed from hydroboration of TBE.[18] We propose this process occurs by way of an initial sacrificial hydrogenation of TBE to form a Rh^I species that then undergoes rapid B-H activation, which in the presence of further TBE follows through to hydroboration. This hydroboration is also catalytic (5 mol%, 0.013 M **3**, ToN 20, three hours) and at the end of catalysis, **3** is recovered as the only organometallic product.

Complex **3** provides a starting point to investigate the reaction of $H_3B{\cdot}NMe_3$ with the Rh^I {Rh(Xantphos)}$^+$ fragment. Addition of excess (20 equivalents) $H_3B{\cdot}NMe_3$ to **3** resulted in the slow (one hour) transformation to form a new complex **4**, alongside **2**, in an approximately 50:50 ratio as measured by NMR spectroscopy (Scheme 4). Free **I** was also released.

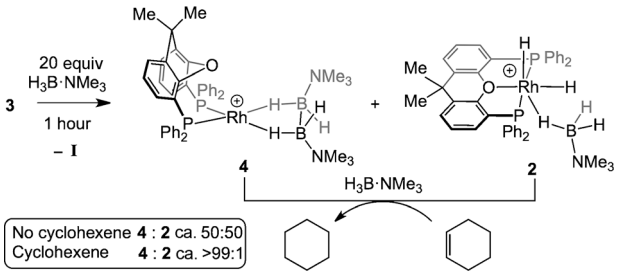

Scheme 4. Synthesis of complex **4**. $[BAr^F_4]^-$ anions not shown.

Complex **4** could be separated from **2** by fractional recystallization and was identified by NMR spectroscopy, ESI-MS, and single-crystal X-ray diffraction as $[Rh(\kappa^2_{P,P}\text{-Xantphos})(\eta^2\text{-}H_4B_2{\cdot}2NMe_3)][BAr^F_4]$. Figure 2 shows the solid-state structure that demonstrates that the homocoupling of two $H_3B{\cdot}NMe_3$ molecules has occurred on the metal center to afford the diborane $H_4B_2{\cdot}2NMe_3$ **II**. The hydrogen atoms of the borane were located and show that coordination with the metal center occurs through two vicinal Rh-H-B interactions,

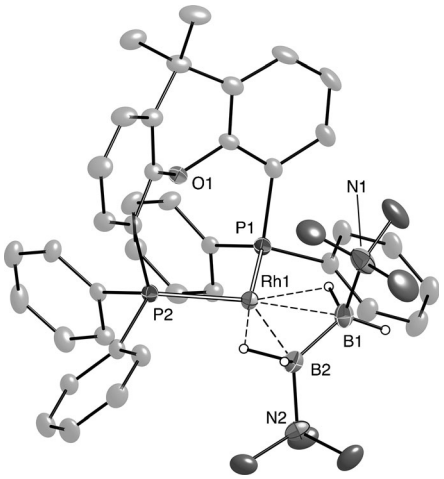

Figure 2. Displacement ellipsoid plots (30%) of the cationic portion of **4**. All carbon-bound hydrogen atoms are omitted for clarity. Selected bond lengths (Å) and angles (°): Rh1–P1, 2.2834(9); Rh1–P2, 2.2720(10); Rh1–B1, 2.405(4); Rh1–B2, 2.411(5); Rh1–O1, 3.304(3); B1–B2, 1.678(7); B1–N1, 1.621(7); B2–N2, 1.619(6); P1–Rh1–P2, 101.56(4); angle between planes: P1Rh1P2/B1B2Rh1, 24.3°.

leading to an eclipsed conformation of the diborane, and thus overall C_1 symmetry. The B–B distance, 1.678(7) Å, is consistent with a single bond, and is shorter than those observed for $Cr(CO)_4(H_4B_2{\cdot}2\,PMe_3)$ (1.748(11) Å)[27] and $[Cu(H_4B_2{\cdot}2\,PMe_3)_2]I$ (1.80(2) Å),[28] which both show similar conformations for the bidentate diborane. In contrast to **4**, these are formed from the preformed diborane and the metal fragment. The cation adopts a Rh^I pseudo-square-planar structure, although the B-B axis is twisted somewhat from being planar with the P_2Rh plane, 24.3°. We propose that this distortion is electronic in origin, to allow for maximal overlap of the bridging Rh-H-B interactions, as calculations on a model Me-Xantphos system (i.e. where the Xantphos Ph groups are replaced with Me substituents) show a similar geometry (Supporting Information). The Rh-B distances (2.405(4), 2.411(5) Å) lie in between those measured in **2** and **3**.

The solution NMR data of **4** are consistent with the gross solid-state structure. However only one environment was observed in the $^{31}P\{^1H\}$ NMR spectrum ($\delta = 26.2$ ppm, J(RhP) 172 Hz); while only two BH ($\delta = 1.51$, -8.47 ppm), one NMe_3, and one Xantphos methyl environment are observed in the ^1H NMR spectrum. This suggests a fluxional process is occurring at room temperature that makes both phosphorus and $\{BH_2NMe_3\}$ groups equivalent. Because two different BH environments are observed (one terminal and one bridging), we discount a mechanism for this that involves dissociation of one Rh-H-B interaction, rotation around the B–B bond, and recoordination.[29] Instead a simple inversion of the Xantphos ligand would account for the observed C_2 symmetry. Such behavior has been noted previously.[30] Cooling a solution (CD_2Cl_2) of **4** to 218 K arrests this process so that, for example, two different Rh-*H*-B ($\delta = -8.02$, -8.55 ppm) and ^{31}P ($\delta = 29.0$ ppm, J(RhP) 164 Hz; $\delta = 28.2$ ppm, J(RhP) 168 Hz) environments are observed, the latter in an ABX pattern. These upfield chemical shifts are also consistent with significant B-H-Rh interactions. Diborane **II** is tightly bound to the metal center, and is not displaced by excess NCMe, similar to $M(CO)_4(H_4B_2{\cdot}2\,PMe_3)$.[27] This also means that the system is not catalytic, because $H_3B{\cdot}NMe_3$ will not displace **II**.

Complex **4** is formed with **2** in approximately equal amounts, alongside **I**, and a mechanism accounting for these transformations, supported by DFT calculations[31] on a model Me-Xantphos system, is shown in Scheme 5. Displacement of

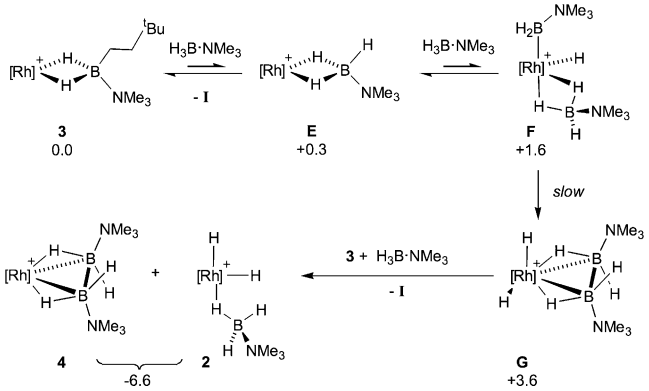

Scheme 5. Proposed key steps in the formation of **4** and **2** from **3**. $[BAr^F_4]^-$ anions not shown. DFT-computed relative free energies are indicated in kcal mol^{-1}. [Rh] = [Rh(Xantphos)] (experimental) or [Rh(Me-Xantphos)] (calculations).

I from **3** by $H_3B{\cdot}NMe_3$ leads to adduct **E** ($G = +0.3$ kcal mol^{-1}). This can undergo rapid, but reversible B-H activation to an initial Rh^{III} hydrido-boryl intermediate that is trapped with excess $H_3B{\cdot}NMe_3$ to give **F** ($G = +1.6$ kcal mol^{-1}). A rate-limiting process that involves B-B coupling then leads to the Rh^{III} intermediate **G** ($G = +3.6$ kcal mol^{-1}), which in the presence of unreacted **3** and excess $H_3B{\cdot}NMe_3$ undergoes ligand redistribution to afford **2** and **4** along with displaced **I**. Complex **2** does not promote B-B coupling and thus the reaction stops. However, addition of excess cyclohexene (which is not hydroborated in this system) to the mixture of **2**, **4**, and excess $H_3B{\cdot}NMe_3$ leads to the generation of a putative Rh^I species, alongside cyclohexane (GC-MS), that can then mediate the coupling (Scheme 4). In this way, nearly quantitative yields of **4** (greater than 99%) can be acheived. The strong binding of **II** in **4** means that it is not displaced by $H_3B{\cdot}NMe_3$, (ΔG for this exchange was calculated to be $+20.6$ kcal mol^{-1}) and thus the system is not catalytic. The structures and bonding in diborane metal complexes of guanidine bases (Scheme 1B) have recently been discussed,[32] in which the bonding was proposed to vary from being dominated by B-H-M interactions to cases where B–B···M bonding prevails (elongation of the B–B bond and only small upfield chemical shift change of the B-H unit). We believe the first description is more accurate here because 1) the B–B distance in **II** was calculated to shorten upon complexation in **4** (from 1.76 Å to 1.70 Å) and 2) an atoms-in-molecules (AIM) analysis of the topology of the electron density in **4** highlighted the presence of bond critical points (bcps) between Rh and the hydrogen atoms bridging the Rh-

B1 and Rh-B2 connectivities. No bcp was located between Rh and either B1 or B2, although a ring critical point was seen between Rh and the center of the B1–B2 bond. The dominance of B-H-M interactions is also consistent with the spectroscopic and structural markers highlighted above for **4**.

Further calculations allow the details of the mechanism outlined in Scheme 5 to be elucidated. Both transformations **E**→**F** and **F**→**G** are multistep processes and the calculations confirmed B-H activation in **E** is more accessible ($\Delta G^{\ddagger} = +8.9$ kcal mol^{-1}) than the subsequent B-B coupling ($\Delta G^{\ddagger} = +27.5$ kcal mol^{-1}). The calculated pathway for the formation of **G** from **F** is shown in Scheme 6. The most stable form of **F**

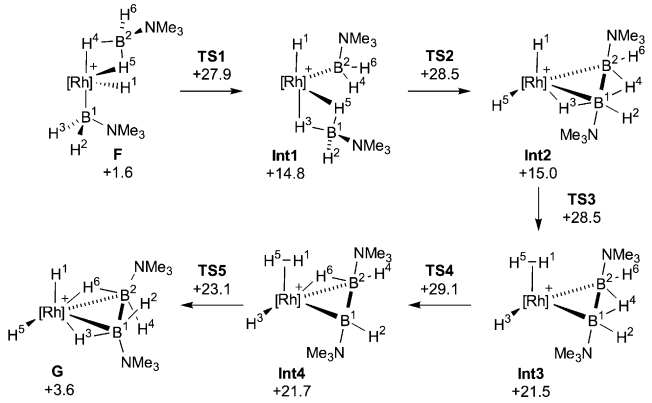

Scheme 6. Computed pathway for formation of **G** from **F** by way of B-B coupling and rearrangement. Calculated free energies (kcal mol^{-1}) are relative to **3** plus two $H_3B{\cdot}NMe_3$ units. [Rh] = [Rh(Me-Xantphos)].

($G = +1.6$ kcal mol^{-1}) has the hydride ligand (H^1) *trans* to one Xantphos arm and isomerisation to move H^1 into an axial position is induced by H^5 transfer between the boron centers. This leads to **Int1** ($G = +14.8$ kcal mol^{-1}) in which the two $\{BH_2NMe_3\}$ fragments are now in a *cis* arrangement. B-B coupling can now occur and is triggered by activation of the B^1-H^5 bond via **TS2** ($G = +28.5$ kcal mol^{-1}) to give dihydride **Int2** ($G = +15.0$ kcal mol^{-1}). The $\{B_2H_4(NMe_3)_2\}$ unit is now established, albeit with bridging hydrides on the Rh-B^1 and B^1-B^2 connectivities. The required rearrangement involves B^1-H^3 bond activation to give the dihydrogen hydride species **Int3** ($G = +21.5$ kcal mol^{-1}). Such reductive coupling of hydride ligands has been noted upon B-H activation of a neighboring amine-borane ligand.[33] H^4 can then shift from a bridging to a terminal position on B^2 and this also induces H^6 to bridge the Rh-B^2 bond (**Int4**, $G = +21.7$ kcal mol^{-1}). B^1-H^3 bond coupling (with concomitant oxidative cleavage of the dihydrogen ligand) completes the formation of **G** ($G = 3.6$ kcal mol^{-1}). B-B coupling therefore proceeds with an overall computed barrier of 29.1 kcal mol^{-1} with the highest-lying transition state corresponding to a rearrangement of the $\{RhB_2H_6(NMe_3)_2\}$ unit (**TS4**) rather than the actual B-B coupling event (**TS2**). Although this barrier is rather high for a process occurring at room temperature, it does include a significant entropic contribution that is likely to be overestimated in the calculations (for example, in **TS2** the $T\Delta S$ term is +13.8 kcal mol^{-1}).[34]

The formation of the final observed products (**2** + **4** + **I**) from **G** (+ **3** + $H_3B{\cdot}NMe_3$) was calculated to be exergonic by 10.2 kcal mol^{-1} (see Scheme 5). A mechanism for this process might involve displacement of **II** in **G** by $H_3B{\cdot}NMe_3$ to give **2**, although this process is rather unfavorable ($\Delta G = +10.2$ kcal mol^{-1}). Alternatively, H_2 loss from **G** would form **4** ($\Delta G = -2.6$ kcal mol^{-1}) with H_2 then reacting with **E** to give **2** ($\Delta G = -7.9$ kcal mol^{-1}). A series of associative ligand displacement processes can also not be discounted. Calculated structures of **2**, **3**, and **4** agree well with the crystallographic data (Supporting Information).

In summary, we report the metal-mediated homocoupling of an amine-borane ($H_3B{\cdot}NMe_3$) that gives a diborane coordinated to a Rh^I center. The mechanism for this process is suggested to operate through sequential B-H activation, the second of these combined with a B–B bond forming step. Aspects of this mechanism might also be generally applicable to related B-N coupling events that lead to dehydropolymerization when using substrates such as $H_3B{\cdot}NMeH_2$. Such a process would require B-H and N-H activation coupled with B–N bond formation and no loss of amino-borane from the metal center, as has been suggested[3,35,36] and shown for the closely related phosphine-borane dehydrocoupling on a Rh^I fragment.[37] Whether a cationic rhodium complex such as **3** catalyzes the dehydropolymerization of $H_3B{\cdot}NMeH_2$ has yet to be reported, but the close similarity to systems that do, such as Ir(*t*BuPOCOP*t*Bu)$(H)_2$, encourages further investigations.

Received: May 21, 2013
Published online: July 19, 2013

Keywords: amine-borane · boron homocoupling · dehydrogenative coupling · rhodium · X-ray diffraction

[1] A. Staubitz, A. P. M. Robertson, I. Manners, *Chem. Rev.* **2010**, *110*, 4079.
[2] A. Staubitz, A. P. M. Robertson, M. E. Sloan, I. Manners, *Chem. Rev.* **2010**, *110*, 4023.
[3] A. Staubitz, M. E. Sloan, A. P. M. Robertson, A. Friedrich, S. Schneider, P. J. Gates, J. Günne, I. Manners, *J. Am. Chem. Soc.* **2010**, *132*, 13332.
[4] For leading references see: L. J. Sewell, G. C. Lloyd-Jones, A. S. Weller, *J. Am. Chem. Soc.* **2012**, *134*, 3598.
[5] H. Braunschweig, R. D. Dewhurst, *Angew. Chem.* **2013**, *125*, 3658; *Angew. Chem. Int. Ed.* **2013**, *52*, 3574.
[6] S. K. Kim, W. S. Han, T. J. Kim, T. Y. Kim, S. W. Nam, M. Mitoraj, L. Piekos, A. Michalak, S. J. Hwang, S. O. Kang, *J. Am. Chem. Soc.* **2010**, *132*, 9954.
[7] E. W. Corcoran, L. G. Sneddon, *J. Am. Chem. Soc.* **1984**, *106*, 7793.
[8] E. W. Corcoran, L. G. Sneddon, *J. Am. Chem. Soc.* **1985**, *107*, 7446.
[9] O. Ciobanu, E. Kaifer, M. Enders, H.-J. Himmel, *Angew. Chem.* **2009**, *121*, 5646; *Angew. Chem. Int. Ed.* **2009**, *48*, 5538.
[10] H. Braunschweig, F. Guethlein, *Angew. Chem.* **2011**, *123*, 12821; *Angew. Chem. Int. Ed.* **2011**, *50*, 12613.
[11] H. Braunschweig, C. Claes, F. Guethlein, *J. Organomet. Chem.* **2012**, *706–707*, 144.
[12] H. Braunschweig, P. Brenner, R. D. Dewhurst, F. Guethlein, J. O. C. Jimenez-Halla, K. Radacki, J. Wolf, L. Zöllner, *Chem. Eur. J.* **2012**, *18*, 8605.
[13] J. Y. Corey, *Adv. Organomet. Chem.* **2004**, *51*, 1.

[14] S. Greenberg, D. W. Stephan, *Chem. Soc. Rev.* **2008**, *37*, 1482.
[15] T. M. Douglas, A. B. Chaplin, A. S. Weller, X. Yang, M. B. Hall, *J. Am. Chem. Soc.* **2009**, *131*, 15440.
[16] M. O'Neill, D. A. Addy, I. Riddlestone, M. Kelly, N. Phillips, S. Aldridge, *J. Am. Chem. Soc.* **2011**, *133*, 11500.
[17] A. B. Chaplin, A. S. Weller, *Angew. Chem.* **2010**, *122*, 591; *Angew. Chem. Int. Ed.* **2010**, *49*, 581.
[18] L. J. Sewell, A. B. Chaplin, A. S. Weller, *Dalton Trans.* **2011**, *40*, 7499.
[19] M. Kranenburg, Y. E. M. van der Burgt, P. C. J. Kamer, P. W. N. M. van Leeuwen, K. Goubitz, J. Fraanje, *Organometallics* **1995**, *14*, 3081.
[20] R. DePoy, G. Kodama, *Inorg. Chem.* **1985**, *24*, 2871.
[21] R. J. Pawley, G. L. Moxham, R. Dallanegra, A. B. Chaplin, S. K. Brayshaw, A. S. Weller, M. C. Willis, *Organometallics* **2010**, *29*, 1717.
[22] For a discussion of binding modes in Xantphos complexes see: G. L. Williams, C. M. Parks, C. R. Smith, H. Adams, A. Haynes, A. J. H. M. Meijer, G. J. Sunley, S. Gaemers, *Organometallics* **2011**, *30*, 6166, and references therein.
[23] N. Merle, G. Koicok-Kohn, M. F. Mahon, C. G. Frost, G. D. Ruggerio, A. S. Weller, M. C. Willis, *Dalton Trans.* **2004**, 3883.
[24] a) A. St. John, K. I. Goldberg, D. M. Heinekey, *Top. Organomet. Chem.* **2013**, *40*, 271; b) A. E. W. Ledger, C. E. Ellul, M. F. Mahon, J. M. J. Williams, M. K. Whittlesey, *Chem. Eur. J.* **2011**, *17*, 8704.
[25] T. J. Hebden, M. C. Denney, V. Pons, P. M. B. Piccoli, T. F. Koetzle, A. J. Schultz, W. Kaminsky, K. I. Goldberg, D. M. Heinekey, *J. Am. Chem. Soc.* **2008**, *130*, 10812.
[26] J. Yang, P. S. White, C. K. Schauer, M. Brookhart, *Angew. Chem.* **2008**, *120*, 4209; *Angew. Chem. Int. Ed.* **2008**, *47*, 4141.
[27] K. Katoh, M. Shimoi, H. Ogino, *Inorg. Chem.* **1992**, *31*.
[28] M. Shimoi, K. Katoh, H. Tobita, H. Ogino, *Inorg. Chem.* **1990**, *29*, 814.
[29] M. Shimoi, K. Katoh, Y. B. Kawano, G. Kodama, H. Ogino, *J. Organomet. Chem.* **2002**, *659*, 102.
[30] A. J. Pontiggia, A. B. Chaplin, A. S. Weller, *J. Organomet. Chem.* **2011**, *696*, 2870.
[31] DFT calculations employed Gaussian 03 and were run with the BP86 functional. See the Supporting Information for full details.
[32] A. Wagner, E. Kaifer, H.-J. Himmel, *Chem. Eur. J.* **2013**, *19*, 7395.
[33] C. J. Stevens, R. Dallanegra, A. B. Chaplin, A. S. Weller, S. A. Macgregor, B. Ward, D. McKay, G. Alcaraz, S. Sabo-Etienne, *Chem. Eur. J.* **2011**, *17*, 3011.
[34] D. Ardura, R. López, T. L. Sordo, *J. Phys. Chem. B* **2005**, *109*, 23618.
[35] H. C. Johnson, A. P. M. Robertson, A. B. Chaplin, L. J. Sewell, A. L. Thompson, M. F. Haddow, I. Manners, A. S. Weller, *J. Am. Chem. Soc.* **2011**, *133*, 11076.
[36] R. T. Baker, J. C. Gordon, C. W. Hamilton, N. J. Henson, P.-H. Lin, S. Maguire, M. Murugesu, B. L. Scott, N. C. Smythe, *J. Am. Chem. Soc.* **2012**, *134*, 5598.
[37] M. A. Huertos, A. S. Weller, *Chem. Sci.* **2013**, *4*, 1881.

